

AD-A120 173

WISCONSIN UNIV-MADISON DEPT OF CHEMISTRY
PHOTOLUMINESCENCE AND ELECTROLUMINESCENCE AS PROBES OF INTERFAC--ETC(U)
SEP 82 H H STRECKERT, J TONG, M K CARPENTER N00014-78-C-0633
UNIS/DC/TR-82/1 NL

UNCLASSIFIED

1 of 1

AD A
120173



END
DATE
FILMED
11-82
DTIC

12

OFFICE OF NAVAL RESEARCH

Contract No. N00014-78-C-0633

Task No. NR 051-690

TECHNICAL REPORT No. UWIS/DC/TR-82/1

Photoluminescence and Electroluminescence as Probes of Interfacial Charge-Transfer Processes Relevant to Cadmium Sulfo-Selenide-Based Photoelectrochemical Cells

by

Holger H. Streckert, Jiu-ru Tong, Michael K. Carpenter and Arthur B. Ellis*

Prepared for Publication

in

"Photoelectrochemistry: Fundamental Processes and Measurement Techniques"; published by The Electrochemical Society, Vol. 82-3; W. L. Wallace, A. J. Nozik, S. K. Deb, and R. H. Wilson, Eds.

Department of Chemistry
University of Wisconsin
Madison, Wisconsin 53706

September 23, 1982

DTIC
ELECTE
OCT 13 1982
S H D

Reproduction in whole or in part is permitted
for any purpose of the United States Government

Approved for Public Release: Distribution
Unlimited

To whom all correspondence should be addressed.

82 10 13 024

AD A120173

DTIC FILE COPY

Unclassified

SECURITY CLASSIFICATION OF THIS PAGE (When Data Entered)

REPORT DOCUMENTATION PAGE		READ INSTRUCTIONS BEFORE COMPLETING FORM
1. REPORT NUMBER UWIS/DC/TR-82/1	2. GOVT ACCESSION NO. A120172	3. RECIPIENT'S CATALOG NUMBER
4. TITLE (and Subtitle) Photoluminescence and Electroluminescence as Probes of Interfacial Charge-Transfer Processes Relevant to Cadmium Sulfo-Selenide-Based Photoelectrochemical Cells	5. TYPE OF REPORT & PERIOD COVERED	
	6. PERFORMING ORG. REPORT NUMBER	
7. AUTHOR(s) Holger H. Streckert, Jiu-ru Tong, Michael K. Carpenter, and Arthur B. Ellis	8. CONTRACT OR GRANT NUMBER(s) N00014-78-C-0633	
9. PERFORMING ORGANIZATION NAME AND ADDRESS Department of Chemistry, University of Wisconsin, Madison, Wisconsin 53706	10. PROGRAM ELEMENT, PROJECT, TASK AREA & WORK UNIT NUMBERS NR 051-690	
11. CONTROLLING OFFICE NAME AND ADDRESS Office of Naval Research/Chemistry Program Arlington, Virginia 22217	12. REPORT DATE September 23, 1982	
	13. NUMBER OF PAGES 20	
14. MONITORING AGENCY NAME & ADDRESS (if different from Controlling Office)	15. SECURITY CLASS. (of this report) Unclassified	
	15a. DECLASSIFICATION/DOWNGRADING SCHEDULE	
16. DISTRIBUTION STATEMENT (of this Report)		
<div style="border: 1px solid black; padding: 5px; display: inline-block;"> This document has been approved for public release and sale; its distribution is unlimited. </div>		
17. DISTRIBUTION STATEMENT (of the abstract entered in Block 20, if different from Report)		
Approved for Public Release - Distribution Unlimited		
18. SUPPLEMENTARY NOTES Prepared for publication in "Photoelectrochemistry: Fundamental Processes and Measurement Techniques"; published by the Electrochemical Society, Vol. 82-3; W. L. Wallace, A. J. Nozik, S. K. Deb, and R. H. Wilson, Eds.		
19. KEY WORDS (Continue on reverse side if necessary and identify by block number) photoluminescence, electroluminescence, cadmium sulfoselenide electrodes <i>Cadmium X is = to</i>		
20. ABSTRACT (Continue on reverse side if necessary and identify by block number) Samples of single-crystal, n-type Cd _{1-x} Se _x (X = 1.00, 0.74, 0.49, 0.26, 0.11, 0.00) emit when excited with ultraband gap excitation. The 295 K band gaps monotonically decrease with X from ~2.4 eV for CdS to ~1.7 eV for CdSe. Photoluminescence (PL) spectra are sharp and have band positions which vary nearly linearly with composition: λ_{max} (nm) = 718-210 X. The energetic proximity to the band gap,		

DD FORM 1473 1 JAN 73

EDITION OF 1 NOV 69 IS OBSOLETE S/N 0102-LF-014-6601

Unclassified

SECURITY CLASSIFICATION OF THIS PAGE (When Data Entered)

Handwritten scribbles

temperature dependence and decay times are all consistent with a description of the PL as edge emission. Measured PL efficiencies, ϕ_r , are 10^{-5} in air. When the samples are used as photoanodes in photoelectrochemical cells (PECs) employing aqueous polysulfide electrolyte, the emission intensity can be quenched by the passage of photocurrent. The extent of quenching can be correlated with the photocurrent quantum efficiency. Electroluminescence (EL) can be initiated by using the $CdS_{(1-x)}Se_x$ samples as dark cathodes in aqueous, alkaline, peroxydisulfate electrolyte at potentials cathodic of ~ 0.9 to -1.1 V vs. SCE. The EL spectral distribution for a given sample is similar to that observed in PL experiments and indicates that the same emissive excited state is involved. At high resolution, EL and PL spectra can differ in a manner which shows evidence of self-absorption effects: The EL spectra are slightly broader than their PL counterparts with the spectral mismatch almost exclusively in the high-energy tail. This suggests that EL occurs, on average, nearer the semiconductor-electrolyte interface. Measured EL efficiencies exceed 10^{-4} ($X = 0.00, 0.11$) or 10^{-5} ($X = 0.26, 0.49, 0.74, 1.00$) at -1.50 V vs. SCE but are smaller near the EL threshold potentials. Comparisons with ϕ_r values are discussed.

Handwritten scribbles

Handwritten scribbles

Accession For	
NTIS GRA&I	<input checked="" type="checkbox"/>
DTIC TAB	<input type="checkbox"/>
Unannounced	<input type="checkbox"/>
Justification	
By	
Distribution/	
Availability Codes	
Dist	Special
A	

copy
inserted

INTRODUCTION

Accompanying the widespread interest in photoelectrochemical cells (PECs) (1) has come a general recognition that techniques are needed for probing the physical properties of semiconductor electrodes, the key component of a PEC. In particular, the dual roles of the semiconductor as photoreceptor and electrode highlight the importance of the interrelationship of the semiconductor's excited-state properties and interfacial charge-transfer processes in the construction of efficient PECs. A very convenient probe for exploring this interrelationship is luminescence: The spectral distribution, intensity and decay time of emitted light provide insight into the constitution and kinetics of the semiconductor's excited-state manifold. Ideally, the emissive features reflect the role of

THE ELECTROCHEMICAL SOCIETY, INC.
CAMERA READY COPY FILING FORM

interfacial charge-transfer events as a form of environmental perturbation.

Two luminescence techniques have been employed in studying semiconductor electrodes. Photoluminescence (PL) has been examined with electrodes of n-type ZnO (2a) and Cu-doped ZnO (ZnO:Cu) (2a,b), CdS:Te and CdS:Ag (2c,d), and p-type GaP (2e). In these PL experiments the excited-state manifold is populated directly by the absorption of light and the effect of introducing photocurrent in the external circuit as a competitive excited-state decay process is determined. A complementary technique is electroluminescence (EL) wherein the excited state is populated by interfacial charge-transfer processes. These studies have been conducted on a host of n-type semiconductors including ZnO (3a), ZnS (3b), ZnSe (3c), GaP (2e,3a,d-f), GaAs (3a,g,h), TiO₂ (3i-k), SnO₂ (3a), SrTiO₃ (3k,l), WO₃ (3k), CdS (3a,m), and CdS:Te (3m). The observation of subband gap EL reported in several cases permitted the identification of intraband gap electronic states.

In this study we characterize the emissive properties of n-type, single-crystal, CdS_xSe_{1-x} ($0 < X < 1$) electrodes. The extreme members of this series, CdS and CdSe, have been used in numerous PEC studies (1) and their ability to form solid solutions of any composition (4) makes them attractive candidates for studying trends in emissive properties as a function of composition. That the mixed solids can be used as photoelectrodes has previously been demonstrated with polycrystalline samples (5). The results presented herein provide an overview of our studies of the PL and EL properties of CdS_xSe_{1-x} samples (6,7). We demonstrate that PL from these electrodes can be perturbed and EL initiated by interfacial charge-transfer processes. In addition, direct comparisons of PL and EL properties are exploited to provide information regarding spatial and mechanistic features of the two kinds of emission.

RESULTS AND DISCUSSION

Samples of n-type, single crystal CdS_xSe_{1-x} representing several values of X were employed for the studies to be described, with CdS and CdSe included as reference points. In the sections which follow we characterize the composition of these samples and their PL and EL properties. PL characterization is based on the spectral distribution and origin of emission, radiative efficiency, and PEC properties. EL characterization includes spectral distribution and efficiency.

Sample Composition. Two methods which have previously been used to characterize the composition of cadmium sulfo-selenide samples are electron microprobe analysis (8) and absorption spectra (9). For the six CdS_xSe_{1-x} samples employed in this study, we found by using an electron microprobe analyzer that X was 1.00, 0.74, 0.49, 0.26, 0.11 and 0.00; we estimate these compositions to be accurate to about 1%. The band gaps of the CdS_xSe_{1-x} compounds are reported to monotonically

THE PHYSICS OF THE CdS_xSe_{1-x} SYSTEM
 CAMERA READY COPY TYPING FORM

decrease with increasing Se content (8-10). We made crude estimates of band gap energies, E_{BG} , from the onsets of absorption spectra (7); for $X = 1.00, 0.74, 0.49, 0.26, 0.11$ and 0.00 , E_{BG} is $\sim 2.37, 2.10, 1.93, 1.80, 1.72$ and 1.68 eV, respectively. These values are in reasonable accord with various estimates reported from measurements of absorption spectra (9), photoconductivity spectra (10a,b), and PEC photoaction spectra (5); plots of E_{BG} (eV) vs. X are in all cases sublinear with respect to a line drawn between the CdS and CdSe E_{BG} end points.

PL Spectra and Origin. When the CdS_xSe_{1-x} samples are irradiated with ultraband gap light, they visibly luminesce. The emitted light is green for $X = 1.00$, yellow-green for $X = 0.74$, orange for $X = 0.49$ and red for the other samples. Typical front-surface emission spectra, obtained in 5M OH⁻ with 457.9 nm Ar ion laser excitation while the samples served as electrodes, are shown in Figure 1a and are quite similar to spectra obtained in air. The bands of all the samples examined are fairly sharp (fwhm values of $\sim 0.05-0.07$ eV) and their positions red-shift with increasing Se content in accord with the observed colors. A plot of the emission band maxima (nm) vs. X approximates the linear relationship of eq. (1); a similar relationship

$$\lambda_{\max} \text{ (nm)} \approx 718-210 X \quad (1)$$

for CdS_xSe_{1-x} ($0 \leq X \leq 1$)

was previously reported in cathodoluminescence and PL studies (8). As noted in the earlier study, eq. (1) permits an independent determination of composition in CdS_xSe_{1-x} samples.

The PL spectra of several samples have breadths which are dependent on excitation wavelength, owing to the overlap of the PL band with the onset of absorption. These self-absorption effects are most apparent in high-resolution spectra of CdSe: its PL spectrum from 457.9 nm excitation is broader than that obtained from ~ 3 -fold more deeply penetrating 632.8 nm excitation (~ 22 -vs. 19-nm fwhm values) with the spectral mismatch occurring almost exclusively in the high-energy tail of the emission band where the probability for reabsorption of the emitted light is greatest (6); more modest but analogous differences are found for several of the other samples (7). Self-absorption effects are also observed in comparisons of PL and EL spectra (vide infra).

The energetic proximity of the emission bands to the band gap region suggests that the PL be described as edge emission (11). Although we are uncertain as to the exact origin of these radiative transitions in our samples, temperature effects and decay times support this description. Cooling the samples to 77 K results in a marked blue-shift of the emission band maxima. The magnitude of these shifts is given in Table I and generally ranges from $\sim 0.07-0.10$ eV. This energetic difference roughly matches the increase in E_{BG} reported for CdS_xSe_{1-x} samples from photoconductivity measurements (10) and supports the notion that the transition is related to E_{BG} . At 77 K we found that several of the samples also exhibited other, weaker

emission bands. These bands are listed in Table I, but we have not characterized them further. Decay times of the six samples were measured at 295 K in air using 337 nm excitation from a N₂ laser and were ≤ 20 ns (7); our measured value for CdSe of ~ 20 ns ($\tau_{1/e}$) is in accord with a recent literature value (12). Decay times in the (sub)-nanosecond regime have been reported for edge emission (13). Taken together, we feel that the energies, temperature dependence and decay times of the observed PL bands are consistent with their classification as edge emission.

PL Efficiency. The PL quantum efficiency, defined as photons emitted per photons absorbed and symbolized by ϕ_r , is difficult to measure accurately. An upper limit to ϕ_r can be obtained for a given set of experimental conditions by finding other conditions which increase its value. As Table I indicates, cooling the CdS_xSe_{1-x} samples to 77 K not only blue-shifts the edge emission band but also markedly increases its intensity. Emission enhancement factors of ~ 20 to 200 correspond to 295 K upper limits on ϕ_r of 0.05 to 0.005; we assume little change in absorbed 457.9 nm intensity in this experiment.

Our second estimate of ϕ_r is based on a technique developed by Wrighton, et al. (14). The "photons absorbed" needed for the ϕ_r calculation is acquired by subtracting the intensity of laser light reflected by the CdS_xSe_{1-x} sample from the intensity reflected by a nonabsorbing standard, a MgO pellet, in the same geometry. This difference is divided into the intensity emitted by the CdS_xSe_{1-x} sample to obtain ϕ_r , after correcting for relative detector response. Typical ϕ_r values are $\sim 10^{-4}$, consistent with the aforementioned upper-limit estimate.

PEC Properties. Although inefficient, luminescence provides insight into the effects of PEC parameters on the excited-state properties of semiconductor electrodes. We constructed one-compartment PECs in the sample compartment of an emission spectrometer. Besides the CdS_xSe_{1-x} photoanode, the PEC consisted of a Pt foil counterelectrode, an SCE, and an aqueous polysulfide electrolyte whose composition was 1 M OH⁻/1M S₂²⁻/0.1 M S. Examination of the front-surface luminescence in these PECs was facilitated by the insensitivity to potential of the emissive spectral distribution (2.0-nm resolution); between the onset of photocurrent and -0.3 V vs. SCE, essentially only the emission intensity changed, permitting it to be monitored by simply sitting at λ_{max} . PL spectra in polysulfide electrolyte were virtually identical to those obtained in OH⁻ electrolyte. The interrelationship of photocurrent, luminescence, and voltage for several CdS_xSe_{1-x}-based PECs is presented in the iLV curves of Figure 2 which were all obtained with 457.9 nm light. At this excitation wavelength the photogenerated electron-hole (e⁻-h⁺) pairs are formed almost exclusively in the depletion region where they are most susceptible to potential-induced changes in band bending (15). Figure 2 reveals that the semiconductor electrodes exhibit decreasing photocurrents and increasing emission intensities with increasingly negative potentials. This inverse relationship is anticipated for what are essentially competitive excited-state deactivation processes: photocurrent is a measure of.....

e^-h^+ pair separation, whereas luminescence is a probe of their recombination. Increasingly negative bias reduces band bending for n-type semiconductors (15); the decreased electric field inhibits e^-h^+ pair separation and promotes their recombination, as illustrated in Figure 2.

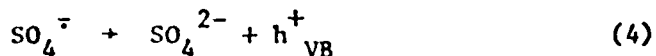
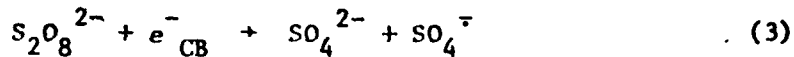
A relationship between photocurrent and emission intensity examined through iLV curves of CdS:Te-based PECs is given by eq. (2) (16,17). The symbols ϕ_x , ϕ_{r_0} , and ϕ_{r_1} represent quantum efficiencies

$$\frac{\phi_{r_0}}{\phi_{r_1}} = \frac{1}{1 - \phi_x} \quad (2)$$

for photocurrent, open-circuit and in-circuit radiative recombination, respectively. The key assumption made in deriving eq. (2) is that the ratio of e^-h^+ pairs recombining radiatively to those recombining nonradiatively is unaffected by potential. The iLV curves of Figure 2, like those of CdS:Te-based PECs, are in reasonable accord with eq. (2). For example, the emission for the X = 0.74 electrode yields a ϕ_{r_0}/ϕ_{r_1} ratio of ~ 15 , using -0.3 V vs. SCE as the ϕ_{r_1} point. From eq. (2) ϕ_x is predicted to be 0.93, in good agreement with the direct measurement of 0.91; the direct measurement is uncorrected for reflection and electrolyte absorption. Similar comparisons for the other iLV curves of Figure 2 are given in Table II and support the applicability of eq. (2) to CdS_XSe_{1-X}-based PECs. Besides luminescence and direct measurement, another complementary technique for determining ϕ_x is photothermal spectroscopy wherein nonradiative recombination (heat) is determined as a function of potential (18); these 3 methods for evaluating ϕ_x have recently been directly compared for ZnO:Cu samples and found to be in good agreement (2b).

Also presented in Table II are energy conversion characteristics of the Figure 2 curves. Monochromatic optical energy conversion efficiencies of ~ 7 -12% were obtained for the single-crystal mixed samples and are comparable to values reported for polycrystalline samples used in similar PECs (5). The onset potential for photocurrent is unusually negative for the X = 0.26 sample and reminiscent of the maximum in a flat-band potential vs. composition curve reported for the polycrystalline samples (5). Although we may be observing a similar trend, our limited sample set presently precludes a definitive conclusion. We should note, however, that the X = 0.26 sample does have a high-energy shoulder in its PL spectrum not seen in the other samples (cf. Table I) and this may be related to its novel i-V properties. One final point regarding the iLV curves is that while no changes were observed after several scans, exchange reactions between the electrode and electrolyte (poly)chalcogenide species have been reported and would be expected to alter the curves over longer experimental periods (19).

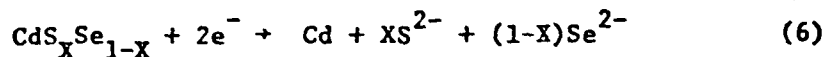
EL Mechanism and Spectra. EL was studied in a N₂-purged, one-compartment cell consisting of a CdS_xSe_{1-x} working electrode, a Pt counter-electrode, an SCE reference electrode and an aqueous, alkaline peroxydisulfate electrolyte (5 M OH⁻/0.1 M S₂O₈²⁻). When sufficiently cathodic potentials were applied to any of the CdS_xSe_{1-x} electrodes, luminescence of the color emitted by that electrode in PL experiments was observed. The mechanism proposed for EL is given in eq. (3)-(5) (2e, 3a, d):



In this scheme an electron in or near the conduction band (e^-_{CB}) reduces S₂O₈²⁻ to yield the strongly oxidizing SO₄^{·-} radical; the radical then injects a hole into or near the valence band (h^+_{VB}). Subsequent radiative recombination yields emission of band gap or subband gap energy. The former case obtains if both the electron and hole are near the band edges; if either or both species are located in intraband gap states such as surface states or dopant states, subband gap emission results.

The redox potentials of eq. (3) and (4) have been estimated to be $\leq +0.6$ and $\geq +3.4$ V vs. NHE, respectively (3d). Initiation of the reaction sequence of eq. (3)-(5) should occur at potentials cathodic of the flat-band potential, E_{FB} , where CdS_xSe_{1-x} samples can serve as dark cathodes. We estimate that E_{FB} values for the samples in aqueous alkaline solution are in the range of ~ -0.7 to -1.0 V vs. SCE. This range is based on values reported for CdS and CdSe and i-V properties of polycrystalline CdS_xSe_{1-x} samples (5,20). Consistent with the postulated E_{FB} position, cathodic current onsets between ~ -0.8 and -1.0 V vs. SCE. For potentials ≥ -1.6 V the current is due predominantly to reduction of S₂O₈²⁻.

Another electrochemical process which can contribute to the observed current is reduction of the electrode to yield surface Cd, eq. (6). This reaction has been reported for CdS in neutral media



and can be photoassisted (21a); evidence for the reaction was the appearance, after reduction, of a sharp anodic stripping peak accompanied by changes in electrode reflectivity (21a) and photoacoustic signal (21b). In OH⁻ or OH⁻/S₂O₈²⁻ electrolytes, we generally did not observe an anodic stripping peak in dark i-V curves (0.0 to -1.5 V) of CdS_xSe_{1-x} samples. That a surface layer might be present, however, was suggested by decays in current and EL intensity which were observed when the CdS_xSe_{1-x} electrodes were brought into circuit in OH⁻ or OH⁻/S₂O₈²⁻ electrolytes at potentials cathodic of ~ -1.2 V. If electrode reduction were occurring, earlier

studies on CdS suggested that anodic cycling might reverse such surface changes (3a,m,21). Evidence that reproducible i-V properties could be obtained in $\text{OH}^-/\text{S}_2\text{O}_8^{2-}$ electrolyte was indicated by pulse experiments: repetitively pulsing the $\text{CdS}_x\text{Se}_{1-x}$ electrodes between 0.0 V (1s) and -1.5 V (1s) gave reproducible coulombs during the cathodic cycle over hundreds of pulses. Additionally, as with CdS (3m) and CdSe (6), little weight loss was found in long-term pulse experiments: For example, a 0.1275 g $\text{CdS}_{0.49}\text{Se}_{0.51}$ sample ($\sim 0.4 \text{ cm}^2$ surface area) showed negligible weight loss after 145 C had been passed in ~ 14 hrs of continuous pulsing between 0.00 V (1s) and -1.50 V (1s) in 10 ml of $\text{OH}^-/\text{S}_2\text{O}_8^{2-}$ electrolyte. Although these results could be ascribed to reversal of electrode reduction during the anodic cycles, any such conclusions await a detailed characterization of the electrochemistry of $\text{CdS}_x\text{Se}_{1-x}$ electrodes in $\text{OH}^-/\text{S}_2\text{O}_8^{2-}$ electrolyte. The possible presence of a surface layer should be kept in mind, however, since it could influence the EL properties to be described.

Placement of the EL cell in the sample compartment of the emission spectrometer permitted EL spectra to be recorded. Threshold potentials for visibly observing EL from the $\text{CdS}_x\text{Se}_{1-x}$ electrodes range from ~ -0.9 to -1.1 V vs. SCE. Because EL intensities generally decayed from their initial value, the pulse technique was employed to obtain EL spectra: $\text{CdS}_x\text{Se}_{1-x}$ electrodes were repetitively pulsed between 0.00 V (11s) and a potential cathodic of the EL threshold potential (1s) while the emission monochromator was slowly scanned. The transient maximum intensities obtained in this procedure were reproducible ($\pm 10\%$) over hundreds of pulses. EL spectra were typically recorded under conditions which facilitated comparisons with PL spectra. For a given sample the PL spectrum was first obtained in air and at -1.50V in OH^- electrolyte. Without disturbing the sample geometry, the electrolyte was changed to $\text{OH}^-/\text{S}_2\text{O}_8^{2-}$ and the EL spectrum obtained by pulsing between 0.00 and -1.50 V vs. SCE. Three representative pairs of EL and PL spectra are given in Figure 1. The similarity of the PL and EL spectra observed for all of our samples indicates that a common emissive excited state is involved in both experiments.

Spectral comparisons made at higher resolution (~ 0.3 nm as opposed to 2.0 nm in Figure 1) often revealed spectral mismatches, as illustrated in Figure 3. The EL spectrum of $\text{CdS}_{0.49}\text{Se}_{0.51}$ is slightly broader than the PL spectrum (fwhm of 22 vs. 20 nm) with the discrepancy occurring almost exclusively in the high-energy tail. We attribute the difference in EL and PL spectra to self-absorption effects. The discrepancy in the breadths of the two spectra of Figure 3 indicates that, on average, EL is produced nearer to the $\text{CdS}_{0.49}\text{Se}_{0.51}$ -electrolyte interface than PL. Similar effects were observed for the other $\text{CdS}_x\text{Se}_{1-x}$ samples with the magnitude of the spectral discrepancy dependent on sample and PL excitation wavelength. Quantifying these inferred differences in EL and PL spatial origins should be possible, in principle, but requires more information than we presently possess. Among the data needed are the spatial

distribution of injected holes, their diffusion length, and evaluation of the role, if any, of a surface layer (vide supra). For the mixed sulfo-selenide samples high-resolution absorption spectra are also needed.

A final point regarding the EL spectra involves subband gap emission. Broad emission bands below the band gap energy have been observed in EL spectra of CdS (3a,m). At the sensitivities used to observe the edge emission, only the EL spectra of the X = 1.00 and 0.74 samples exhibited subband gap emission at $\lambda \leq 800$ nm. As described above, the presence of subband gap emission implicates the involvement of intraband gap states in the radiative transition. Although these states are presently uncharacterized for the systems at hand, our inability to detect the corresponding emission bands in PL experiments conducted under similar conditions (5M OH⁻ electrolyte; -1.50 V vs. SCE) is noteworthy. We found that homogeneously doped samples of CdS:Te exhibited subband gap emission in both PL and EL spectra (3m). The observed difference in PL and EL spectra for the X = 1.00 and 0.74 samples may reflect an inhomogeneous distribution of the intraband gap states. In particular, localization of the intraband gap states at or near the surface (surface states, e.g.) would make detection of the corresponding emission easier in an EL experiment, if EL were significantly more surface-sensitive than PL. Although our data suggests that this might be the case, additional experiments are needed to prove it conclusively.

EL Efficiency. We have adapted measures of efficiency from studies of electrogenerated chemiluminescence (ecl) to make estimates of EL efficiency (22). Integrated EL efficiencies, $\bar{\phi}_{EL}$, were determined by the pulse technique described earlier in conjunction with eq. (7); F is Faraday's constant. Total emitted light was estimated by placing

$$\bar{\phi}_{EL} = \frac{\text{total emitted light (einsteins)} \times F}{\text{total coulombs due to hole injection}} \quad (7)$$

a radiometer next to the sole exposed face of the emitting electrode. The integrated energy in a single-pulse experiment (μ J) was converted to einsteins at λ_{max} of the emission band for each of the CdS_XSe_{1-X} samples; the sharpness of the bands makes this a reasonable approximation. Since not all of the photons are collected in this procedure, the value used for the numerator of eq. (7) is a lower limit. The denominator of eq. (7) was obtained by using a digital coulometer to integrate the coulombs over the single pulse. Because we use total coulombs for the calculation and not the coulombs due to hole injection, we are likely overestimating the denominator of eq. (7). If equations (3)-(5) are mechanistically correct, for example, our use of total coulombs is too large by a factor of two. Additionally, we have not corrected for background coulombs obtained in the absence of S₂O₈²⁻, although this is at most a few percent for potentials ≥ -1.5 V vs. SCE. The combination of underestimated numerator and overestimated denominator in eq. (7) yields $\bar{\phi}_{EL}$ estimates which should be treated as lower-limit estimates.

Table III presents a compilation of $\bar{\phi}_{EL}$ values near the EL threshold potential and at -1.50 V vs. SCE for the CdS_xSe_{1-x} samples. At -1.50 V the EL efficiencies range from $\sim 10^{-5}$ to in excess of 10^{-4} with the two samples having the highest Se content consistently giving the largest $\bar{\phi}_{EL}$ values. Modest declines in $\bar{\phi}_{EL}$ (generally, factors of ≤ 10) are observed in passing to the threshold potential, although the constituents of $\bar{\phi}_{EL}$ (μJ , coulombs) often decreased by much larger factors.

Comparisons of ϕ_r and $\bar{\phi}_{EL}$ are noteworthy but must be made with care. The value of ϕ_r measured in air for the CdS_xSe_{1-x} samples, $\sim 10^{-4}$, is comparable to the $\bar{\phi}_{EL}$ values of Table III. A more meaningful comparison can be made, however, if ϕ_r is determined in OH^- electrolyte at the same potentials used in EL experiments. We found for CdSe, in fact, that lower-limit estimates of ϕ_r were larger, $\sim 1 \times 10^{-3}$ at -1.50 V in 5 M OH^- , but that this value dropped by a factor of ~ 3 by -0.9 V (6). Similar trends in emitted intensity (and therefore in ϕ_r if absorbed intensity is unperturbed by potential) were shown by the other CdS_xSe_{1-x} samples. This decline with anodic potential is similar to the trend in measured $\bar{\phi}_{EL}$ values with potential. Such a relationship is intriguing because, by analogy with ecl studies (22), $\bar{\phi}_{EL}$ can be factored into an efficiency for excited-state population, ϕ_{ES} (excited states populated per holes injected), and the radiative efficiency, ϕ_r (photons emitted per excited states populated). Although the uncertainties in ϕ_r and $\bar{\phi}_{EL}$ preclude a more precise comparison, it is tempting to conclude that ϕ_{ES} is very large, perhaps approaching its maximum value of unity, over the potential range examined. However, the different spatial origins for PL and EL inferred from their spectra suggest caution in comparing efficiencies, even when ϕ_r and $\bar{\phi}_{EL}$ are known with certainty. Strictly speaking, PL and EL efficiencies should only be compared in the same spatial regions of the electrode, since ϕ_r values may be region dependent because of local variations in environment. The solid-liquid interface is a particularly important environment for EL, since it is the region in which EL is initiated and EL appears to occur, on average, nearer to it than PL. We have, in fact, seen substantial discrepancies in our estimates of $\bar{\phi}_{EL}$ and ϕ_r near the EL threshold potential for CdSe and this could be attributed to changes in ϕ_{ES} and/or ϕ_r resulting from altered (near-)surface conditions (6). Evidence that (near-)surface contributions to PL can be enhanced was obtained through PEC etching (23). With this technique the photo-anodic decomposition of CdSe was permitted to occur; subsequently the CdSe PL spectrum was more intense and broader in its high-energy tail, consistent with a greater PL contribution from (near-)surface regions where self-absorption is minimized (6). To summarize this section, until the spatial dependence of ϕ_{ES} and ϕ_r can be determined more accurately, only limited comparisons between EL and PL efficiencies can be made.

In conclusion, we feel that this study demonstrates useful applications of luminescence to the characterization of $\text{CdS}_x\text{Se}_{1-x}$ electrodes. Perturbation of PL and initiation of EL through interfacial charge-transfer processes is shown to be a general feature of these materials and provides insight into the population and deactivation of the electrodes' emissive excited states. Comparisons of PL and EL spectral distributions and efficiencies highlight spatial and mechanistic features of the two kinds of emission. Experiments to better understand the interrelationship of PL, EL and charge-transfer events are in progress.

EXPERIMENTAL

Materials. Single-crystal c-plates (10x10x1 mm) of n-type $\text{CdS}_x\text{Se}_{1-x}$ ($x = 1.00, 0.74, 0.49, 0.26, 0.11, \text{ and } 0.00$) were obtained from Cleveland Crystals, Cleveland, Ohio. The crystals were vapor-grown with resistivities of ~ 2 ohm-cm. After being cut to dimensions of $\sim 0.25 \text{ cm}^2 \times 1 \text{ mm}$, the samples were etched in Br_2/MeOH (1:10 v/v) and mounted as electrodes as described previously (2d). The preparation of polysulfide and peroxydisulfate electrolytes has also been described (2d,3m). MgO powder was obtained from Baker Chemical Co., $\text{MnBr}_2 \cdot 4\text{H}_2\text{O}$ from Aldrich, Et_4NBr from Eastman.

Optical Measurements. Uncorrected emission spectra were taken with an Aminco-Bowman spectrophotofluorometer (200-800 nm; band width ~ 1.0 or 2.0 nm) equipped with a Hamamatsu R446S red-sensitive PMT. A McPherson Model 270, 0.35-m monochromator, equipped with both a grating blazed at 500 nm and the R446S PMT, was employed for high-resolution (~ 0.3 nm bandwidth) spectra. A grating blazed at 1000 nm and an EMI model 9684B PMT (S-1 response) extended the spectral range to 1100 nm. Signals from either PMT used in the McPherson-based spectrometer were amplified by a Keithley Model 414S picoammeter and displayed on a Houston Model 2000 x-y recorder. The 457.9 and 514.5 nm lines of a Coherent Radiation CR-12 Ar ion laser and the 632.8 nm line of a CR-80 He-Ne laser were used for excitation. The 2-3 mm diameter Ar ion laser beam was 10X expanded, passed through appropriate filters to eliminate plasma lines, and often masked to fill the sample surface area; laser excitation was filtered in emission spectral measurements with suitable filters placed in front of the PMT (7). Laser intensity, adjusted by changing the power or by neutral density filters, was measured with a Scientech 362 power energy meter (flat response, 250-35,000 nm) or a Tektronix J16 radiometer equipped with a J6502 probe head (flat response, 450-950 nm). An EG & G Model 550-1 radiometer (flat response, 460-975 nm) equipped with a Model 550-3 pulse integration module was used for integrated energy measurements of the light produced in pulse EL experiments. A quartz disk was used as a beam splitter during experiments requiring continuous monitoring of laser intensity.

Sample Composition. Absorption spectra were obtained from samples which had been polished sequentially with 5.0- and 1.0- μm alumina.

PHOTOCURRENT QUANTUM EFFICIENCY, P.C.
 CdS_xSe_{1-x} BY COMPARING TO CdSe

Samples were placed in a metal holder which restricted the optical window to a ~ 2 mm diameter hole. X-ray analyses were performed on a Bausch & Lomb ARL SEMQ electron microprobe. Samples were ohmically contacted with Ga/In eutectic and Ag epoxy to Al discs. The crystals were mechanically fastened with epoxy and polished with 1.0 μm alumina to obtain flat samples. The primary electron beam energy of 15 keV yielded a sample current of 20 nA. All concentrations were corrected by a standard ZAF correction program. At least 5 regions of each sample were examined to establish sample homogeneity.

PL Properties. Front-surface PL spectra were generally obtained by positioning the sample at $\sim 45^\circ$ to both the Ar ion laser beam and the emission detection optics. The spectral mismatch described in the text was observed for several sample geometries including "head on" excitation along the c-axis (vide infra) and, for some samples, also using the He-Ne laser for 632.8 nm excitation. Spectra were taken both in air and with the samples serving as electrodes in 5 M OH⁻ at various potentials. Spectra at 77 K were obtained by placing samples in a liquid N₂-cooled quartz Dewar which was positioned in the sample compartment of the Aminco-Bowman spectrometer as described previously (2d); spectra beyond 800 nm were taken on the McPherson-based spectrometer. Relative emission intensities between 295 and 77 K which were needed for upper-limit radiative efficiencies, ϕ_r , were corrected for relative detector response (6,7). A second estimate of ϕ_r was made by "head on" irradiation of the CdS_xSe_{1-x} samples and MgO in a quartz cuvette positioned in the Aminco-Bowman spectrometer's sample compartment as previously described (14). The difference in areas of the reflected light between MgO and the CdS_xSe_{1-x} sample represents photons absorbed by the semiconductor and is divided into the area under the emission band, representing photons emitted. Both the absorbed and emitted intensities are corrected for relative detector response. The salt [Et₄N]₂[MnBr₄], prepared as described in the literature (24), served as a standard and gave a ϕ_r value similar to that previously reported (14). Decay times for CdS_xSe_{1-x} samples were obtained in air with 337 nm excitation using instrumentation and techniques previously reported (25). Peak intensities of ~ 3 and 30 kW/cm² were used with essentially no difference in the resulting decay curves. PEC etching procedures used on CdSe have been described (6).

PEC Experiments. A cell suitable for conducting PEC studies in polysulfide electrolyte has been described (2d). Potentiostatic iLV curves were obtained using a PAR Model 173 potentiostat/galvanostat, a Model 175 programmer, and a Model 179 digital coulometer/I to E converter; the techniques used to generate these curves and to measure photocurrent quantum efficiency have been reported (2d). The Aminco-Bowman spectrometer (2.0-nm resolution) was used exclusively for obtaining iLV data with the emission intensity monitored at the emission band maxima of the CdS_xSe_{1-x} samples. Current-voltage curves relevant to EL studies were taken in both 5 M OH⁻ and 5 M OH⁻/0.1 M S₂O₈²⁻. Electrolytes were stirred by a N₂-purge.

EL Spectra. Pulse EL spectra were obtained in both the Aminco-Bowman and McPherson-based spectrometers; experiments in the Aminco-Bowman

THE ELECTROCHEMICAL SOCIETY, INC.
CAMERA READY COPY TYPING FORM

instrument have been described previously (3m). Pulsing the electrode between 0.00 V (11s) and potentials cathodic of ~ -1.0 V (1s) gave sufficiently intense and reproducible transient signals (recorder response time of 0.3 s) to permit the EL spectrum to be obtained as a series of vertical lines as the emission monochromator was swept. Direct comparisons of EL and PL spectra were made for the $\text{CdS}_x\text{Se}_{1-x}$ compounds: For each sample the PL spectrum was obtained in air and in 5 M OH^- electrolyte at -1.50 V vs. SCE. Without disturbing the geometry the EL spectrum was then taken in 5 M $\text{OH}^-/0.1$ M $\text{S}_2\text{O}_8^{2-}$ solution (6,7). These comparisons were made under both low- and high-resolution conditions (*vide supra*).

EL Efficiency. The integrated EL efficiency, ϕ_{EL} , was estimated by placing the probe head of the EG & G radiometer as close as possible (within ~ 1 cm) to the sole exposed $\text{CdS}_x\text{Se}_{1-x}$ crystal face (6,7). The electrode was pulsed to a given potential for 1s as described above and the total emitted energy (in μJ) per pulse measured with the EG & G Model 550-3 accessory. Total coulombs passed during the pulse were measured with the digital coulometer. These measurements were repeated as a function of potential. Relative PL intensity as a function of potential (457.9 nm excitation) was obtained in 5 M OH^- electrolyte for comparison with ϕ_{EL} . PL intensity was monitored at λ_{max} of the $\text{CdS}_x\text{Se}_{1-x}$ sample while the electrode potential was swept between -0.90 and -1.50 V vs. SCE at 20 mV/s.

Acknowledgment. This work was generously supported by the Office of Naval Research. Financial support for J.-R.T. as a visiting scholar at the UW-Madison by the People's Republic of China is greatly appreciated. A.B.E. gratefully acknowledges support as an Alfred P. Sloan Fellow (1981-1983). We thank Dr. E. D. Glover for assistance with the electron microprobe measurements.

REFERENCES

- (1) (a) A. J. Bard, Science, **207**, 139 (1980); (b) M. S. Wrighton, Acc. Chem. Res., **12**, 303 (1979); (c) A. J. Nozik, Ann. Rev. Phys. Chem., **29**, 189 (1978).
- (2) (a) G. Petermann, H. Tributsch, and R. Bogomolni, J. Chem. Phys., **57**, 1026 (1972); (b) A. Fujishima, Y. Maeda, and K. Honda, Abstract No. 502, 160th Meeting of the Electrochemical Society, Inc., October, 1981 and Chem. Lett., submitted for publication; (c) A. B. Ellis and B. R. Karas, Adv. Chem. Ser., **184**, 185 (1980); (d) B. R. Karas and A. B. Ellis, J. Am. Chem. Soc., **102**, 968 (1980); (e) K. H. Beckmann and R. Memming, J. Electrochem. Soc., **116**, 368 (1969).
- (3) (a) B. Pettinger, H.-R. Schöppel, and H. Gerischer, Ber. Bunsenges phys. Chem., **80**, 849 (1976); (b) L. J. Van Ruyven and F. E. Williams, Phys. Rev. Lett., **16**, 889 (1966); (c) J. Gautron, J. P. Dalbera, and P. Lemasson, Surf. Sci., **99**, 300 (1980); (d) R. Memming, J. Electrochem. Soc., **116**, 785 (1969); (e) R. Memming and G. Schwandt, Electrochim. Acta, **13**, 1299 (1968); (f) R. Memming and F. Möllers, Ber. Bunsenges phys. Chem., **76**, 609 (1972);

THE ELECTROCHEMICAL SOCIETY
CAMERA READY COPY INSTRUCTIONS

- (g) D. J. Benard and P. Handler, Surf. Sci., **40**, 141 (1973);
(h) H. Gerischer, N. Müller, and O. Haas, J. Electroanal. Chem.,
119, 41 (1981); (i) R. N. Noufi, P. A. Kohl, S. N. Frank, and
A. J. Bard, J. Electrochem. Soc., **125**, 246 (1978); (j) H. Morisaki
and K. Yazawa, Appl. Phys. Lett., **33**, 1013 (1978); (k) H. Morisaki
H. Kitada, and K. Yazawa, Jpn. J. App. Phys., **19**, 679 (1980);
(l) J. G. Mavroides, Proc. Electrochem. Soc., **77-3**, 84 (1977);
(m) H. H. Streckert, B. R. Karas, D. J. Morano and A. B. Ellis,
J. Phys. Chem., **84**, 3232 (1980).
- (4) N. I. Vitrikhouskii and I. B. Mizetskaya, in "Growth of Crystals,"
Vol. 3, p. 247, Consultants Bureau, New York (1962).
- (5) R. N. Noufi, P. A. Kohl, and A. J. Bard, J. Electrochem. Soc.,
125, 375 (1978).
- (6) H. H. Streckert, J. Tong, and A. B. Ellis, J. Am. Chem. Soc.,
in press.
- (7) H. H. Streckert, J. Tong, M. K. Carpenter, and A. B. Ellis,
J. Electrochem. Soc., in press.
- (8) G. Oelgart, R. Stegmann, and L. John, Phys. Stat. Sol. A., **59**,
27 (1980).
- (9) (a) F. L. Pedrotti and D. C. Reynolds, Phys. Rev., **127**, 1584
(1962); (b) E. T. Handelman and W. Kaiser, J. Appl. Phys., **35**,
3519 (1964).
- (10) (a) R. H. Bube, J. Appl. Phys., **35**, 586 (1964); (b) Y. S. Park,
and D. C. Reynolds, Phys. Rev., **132**, 2450 (1963); (c) R. H.
Bube, Phys. Rev., **98**, 431 (1955).
- (11) R. E. Halsted in "Physics and Chemistry of II-VI Compounds,"
M. Aven and J. S. Prener, Editors, Chapter 8, North-Holland
Publishing Co., Amsterdam (1967).
- (12) Z. Harzion, N. Croitoru, and S. Gottesfeld, J. Electrochem. Soc.,
128, 551 (1981).
- (13) W. Lehmann, Solid-State Electronics, **9**, 1107 (1966).
- (14) M. S. Wrighton, D. S. Ginley, and D. L. Morse, J. Phys. Chem.,
78, 2229 (1974).
- (15) H. Gerischer, J. Electroanal. Chem., **58**, 263 (1975).
- (16) B. R. Karas, D. J. Morano, D. K. Bilich, and A. B. Ellis,
J. Electrochem. Soc., **127**, 1144 (1980).
- (17) A. B. Ellis, B. R. Karas, and H. H. Streckert, Faraday Discuss.
Chem. Soc., **70**, 165 (1980).
- (18) (a) G. H. Brilmyer, A. Fujishima, K. S. V. Santhanam, and A. J.
Bard, Anal. Chem., **49**, 2057 (1977); (b) A. Fujishima, Y. Maeda,
K. Honda, G. H. Brilmyer, and A. J. Bard, J. Electrochem. Soc.,
127, 840 (1980); (c) A. Fujishima, H. Masuda, K. Honda, and
A. J. Bard, Anal. Chem., **52**, 682 (1980); (d) G. H. Brilmyer and
A. J. Bard, Anal. Chem., **52**, 685 (1980).
- (19) D. Cahen, B. Vainas, and J. M. Vandenberg, J. Electrochem. Soc.,
128, 1484 (1981) and references therein.
- (20) (a) A. B. Ellis, S. W. Kaiser, J. M. Bolts, and M. S. Wrighton,
J. Am. Chem. Soc., **99**, 2839 (1977); (b) T. Watanabe, A. Fujishima,
and K. Honda, Chem. Lett., 897 (1974).

ELECTROCHEMICAL SOCIETY, INC.
CAMERA READY COPY TYPING FORM

- (21) (a) D. M. Kolb and H. Gerischer, Electrochim. Acta, 18, 987 (1973); (b) H. Masuda, A. Fujishima, and K. Honda, Chem. Lett., 1153 (1980).
- (22) (a) A. J. Bard, C. P. Keszthelyi, H. Tachikawa, and N. E. Tokel in "Chemiluminescence and Bioluminescence," M. J. Cormier, D. M. Hercules and J. Lee, Eds. pp. 193-208, Plenum Press, New York (1973); (b) L. R. Faulkner and A. J. Bard, Electroanal. Chem., 10, 1 (1977); (c) C. P. Keszthelyi, N. E. Tokel-Takvoryan, and A. J. Bard, Anal. Chem., 47, 249 (1975).
- (23) (a) R. Tenne and G. Hodes, Appl. Phys. Lett., 37, 428 (1980); (b) R. Tenne, Ber. Bunsenges. phys. Chem., 85, 413 (1981); (c) C. J. Liu, J. Olsen, D. R. Saunders, and J. H. Wang, J. Electrochem. Soc., 128, 1224 (1981).
- (24) N. S. Gill and F. B. Taylor, Inorg. Syn., 9, 136 (1967).
- (25) B. R. Karas, H. H. Streckert, R. Schreiner, and A. B. Ellis, J. Am. Chem. Soc., 103, 1648 (1981).

Table I. Temperature Dependence of Photoluminescence Spectra^a

CdS _x Se _{1-x} Sample, X	λ_{max} , nm(eV) ^b		Spectral Shift, eVc	Intensity Enhancement ^d
	295 K	77 K		
1.00 (CdS)	*508 (2.44)	*488 (2.54)	0.10	50
		502 sh (2.47)		
		510 sh (2.43)		
		592 (2.09)		
0.74	*563 (2.20)	*545 (2.27)	0.07	200
		555 sh (2.23)		
0.49	*615 (2.02)	*591 (2.10)	0.08	200
		604 sh (2.05)		
0.26	600 sh (2.06) ^f	600 sh (2.06) ^f	0.08	30
	*663 (1.87)	*636 (1.95)		
		672 (1.84)		
		786 (1.58)		
		*665 (1.86)		
0.11	*695 (1.78)	*665 (1.86)	0.08	100
		680 sh (1.82)		
		850 (1.46) ^e		
0.00 (CdSe)	*718 (1.73)	*681 (1.82)	0.09	20
		698 sh (1.78)		
		830 (1.49) ^e		

- a. Properties of uncorrected PL spectra of CdS_xSe_{1-x} samples excited with 457.9 nm excitation. Spectra were recorded at 295, 77, and 295 K again to demonstrate reproducibility.
- b. Emission band maxima at 295 and 77 K. The band assigned as edge emission is denoted by an asterisk; shouldered are indicated by "sh". Spectral resolution was ~2.0 nm.
- c. Spectral shift between 295 and 77 K for the edge emission band maxima.
- d. Factor by which the emitted intensity of the edge emission band increased on cooling from 295 to 77 K. This factor has been corrected for relative detector sensitivity.
- e. Recorded using the McPherson-based spectrometer (see Experimental).
- f. This band, which exceeds the edge emission band in energy, is noteworthy (see text). It shows little change in energy or intensity on cooling to 77 K and is also observed in EL experiments.

Table II. Measurements of Efficiency in Luminescent CdS_XSe_{1-X}-Based PECs^a

CdS _X Se _{1-X} Electrode, X	ϕ_{r_0} / ϕ_{r_1} ^b	ϕ_x ^c calc.	ϕ_x ^c meas.	ϕ_x at η_{max} ^e	E_y at η_{max} , V ^f	V_{on} , V ^g vs SCE	η_{max} , % ^h
1.00 (CdS)	1.7	0.41	0.37	0.30	0.42	-1.37	4.6
0.74	15	0.93	0.91	0.63	0.42	-1.38	9.7
0.49	7.8	0.87	0.86	0.55	0.35	-1.38	7.1
0.26	16	0.94	0.93	0.63	0.47	-1.52	12
0.11	37	0.97	0.90	0.58	0.34	-1.42	7.3
0.00 (CdSe)	51	0.98	0.86	0.65	0.39	-1.40	9.3

- a. PEC characterization parameters extracted from the iV curves of Figure 2; data for the X = 0.26 sample not pictured in Figure 2 are also included. The indicated crystal served as the photoanode in a PEC employing N₂-purged 1 M OH⁻/1 M S²⁻/0.1 M S polysulfide electrolyte; a Pt foil counterelectrode and SCE completed the PEC. Electrodes were irradiated with ~1.0 to 1.2 mW of 457.9 nm excitation; their exposed surface areas were ~0.25 cm².
- b. Ratio of open-circuit to in-circuit emission intensity with the in-circuit value taken at -0.30 V vs. SCE. Emission intensity was monitored at the edge emission band maximum.
- c. Photocurrent quantum efficiency at -0.30 V vs. SCE calculated from the ϕ_{r_0}/ϕ_{r_1} ratio in the preceding column and eq. (2) in the text.
- d. Measured photocurrent quantum efficiency at -0.30 V vs. SCE determined with a radiometer. 2d Measured values are uncorrected for reflection and electrolyte absorption.
- e. Measured photocurrent quantum efficiency at the potential where maximum optical to electrical energy conversion efficiency obtains.
- f. Output voltage at the maximum energy conversion point. The redox potential of the polysulfide electrolyte was -0.78 V vs. SCE.
- g. The potential at which the onset of anodic photocurrent occurs.
- h. (Maximum electrical power out divided by input optical power) x 100.
- i. The electrolyte pathlength was visibly longer for this electrode than for the others and would, therefore, require a larger correction for electrolyte absorption.

Table III. Estimates of Electroluminescence Efficiency^a

CdS _x Se _{1-x} Electrode, X	Potential, V vs. SCE ^b	Total emitted light μJ (10 ¹² einsteins) ^c	10 ³ total Coul (10 ⁸ mole e ⁻) ^d	10 ⁴ $\frac{e}{\Phi_{EL}}$
1.00 (CdS)	-1.50	0.11 (0.49)	3.4 (3.5)	0.14
	-1.05	0.00063 (0.0027)	0.049 (0.050)	0.054
0.74	-1.50	0.23 (1.1)	6.8 (7.1)	0.15
	-1.00	0.0029 (0.014)	0.61 (0.63)	0.023
0.49	-1.50	0.61 (3.2)	9.7 (10.1)	0.32
	-1.00	0.0014 (0.0073)	0.080 (0.083)	0.088
0.26	-1.50	0.29 (1.6)	4.7 (4.9)	0.33
	-1.00	0.0012 (0.0066)	0.56 (0.58)	0.011
0.11	-1.50	1.2 (7.1)	5.7 (5.9)	1.2
	-1.00	0.036 (0.21)	0.40 (0.42)	0.51
0.00 (CdSe)	-1.50	5.6 (34)	7.0 (7.2)	4.7
	-1.00	0.056 (0.34)	0.53 (0.55)	0.62

- a. A single-crystal, n-type CdS_xSe_{1-x} sample was used as the working electrode in a one-compartment EL experiment conducted in a N₂-purged 5 M NaOH/0.1 M K₂S₂O₈ electrolyte; a Pt foil counter-electrode and SCE completed the cell. The CdS_xSe_{1-x} exposed surface areas were ~0.25 cm².
- b. EL experiments conducted by pulsing the CdS_xSe_{1-x} electrode between 0.00 V (11s) and the indicated potential (1s).
- c. Total emitted light collected per pulse with a radiometer operated in its integrating mode. The radiometer was placed ~1 cm away from the emitting electrode. If all of the indicated energy were converted to photons at the emission band maxima (508, 563, 615, 663, 695 and 718 nm for X = 1.00, 0.74, 0.49, 0.26, 0.11, and 0.00, respectively), the quantity of einsteins given in parentheses would be obtained.
- d. Total coulombs collected per pulse with a digital coulometer. The value in parentheses is the corresponding quantity of electrons in the external circuit, obtained by dividing the coulombs by Faraday's constant.
- e. Integrated EL efficiency from eq. (7) and entries in preceding columns. Each value is the average of at least 5 pulse sequences.

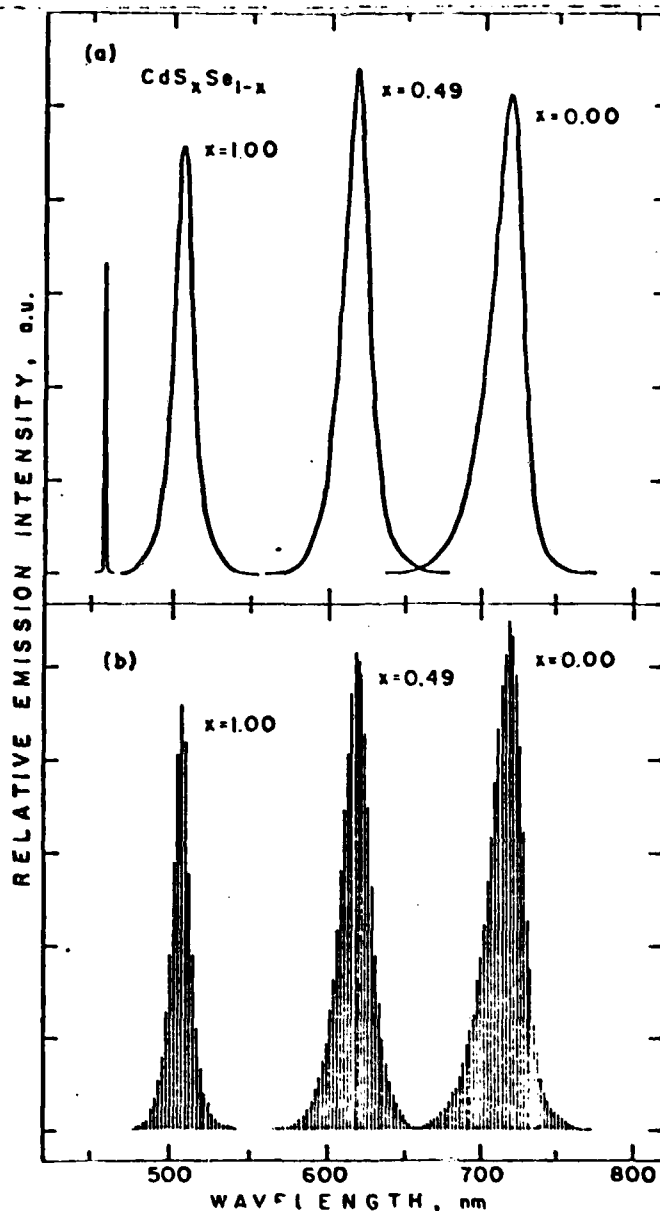


Figure 1. (a) Uncorrected PL spectra of $\text{CdS}_x\text{Se}_{1-x}$ samples irradiated in 5 M OH^- electrolyte while held at -1.50 V vs. SCE. The $\sim 0.25\text{-cm}^2$ samples were excited with ~ 1.0 mW of 457.9 nm light (excitation spike shown at 1/100 the scale of the PL spectrum). PL intensities are not directly comparable because of geometry differences. (b) Uncorrected EL spectra of the samples in (a) obtained without changing their geometry. The EL electrolyte was 5 M $\text{OH}^-/0.1$ M $\text{S}_2\text{O}_8^{2-}$. Electrodes were continuously pulsed between 0.00 V (11s) and -1.50 V vs. SCE (1s) while the spectrometer was scanned (12 nm/min). For both PL and EL a spectral resolution of 2.0 nm was employed.

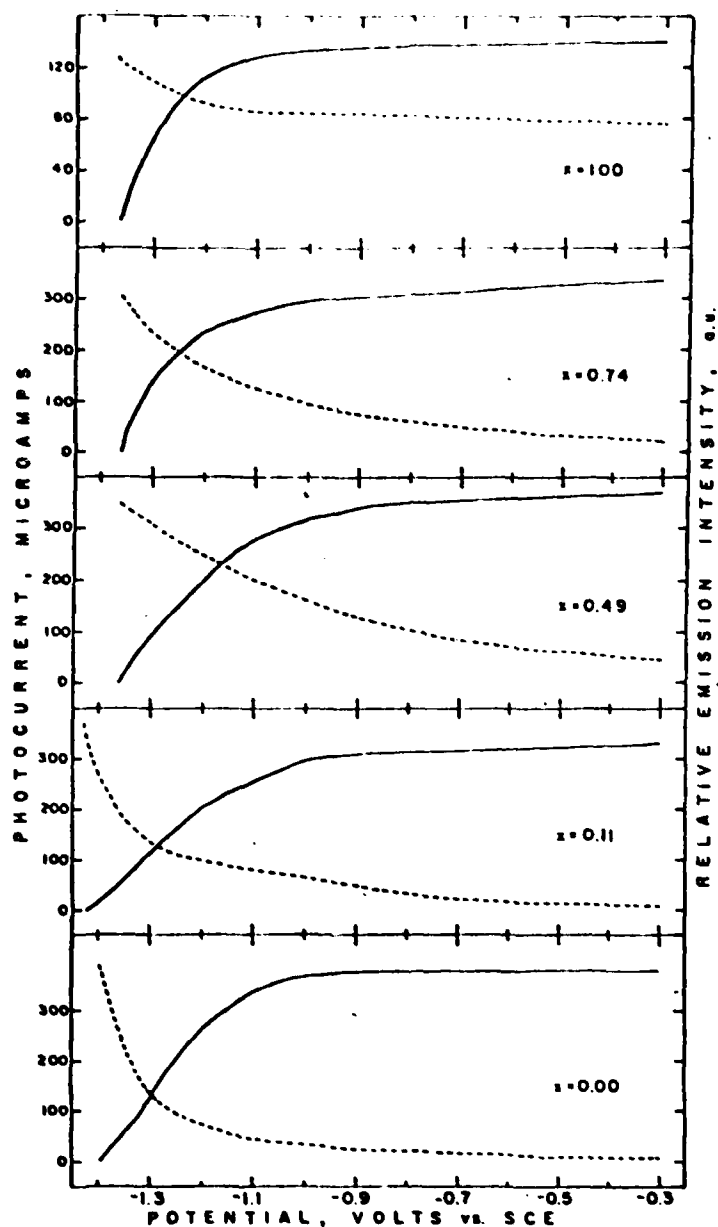


Figure 2. Photocurrent (solid lines, left-hand scales) and emission intensity (dashed lines, right-hand scales) monitored at emission band maxima for five single-crystal $\text{CdS}_x\text{Se}_{1-x}$ electrodes in $1\text{ M OH}^-/1\text{ M S}^{2-}/0.1\text{ M S}$ electrolyte as a function of potential. The electrodes ($\sim 0.25\text{-cm}^2$ exposed area) were excited with $\sim 1.0\text{-}1.2\text{ mW}$ of 457.9 nm light from a beam-expanded Ar ion laser. These iLV curves were swept at 10 mV/s . The electrolyte redox potential was -0.78 V vs. SCE .

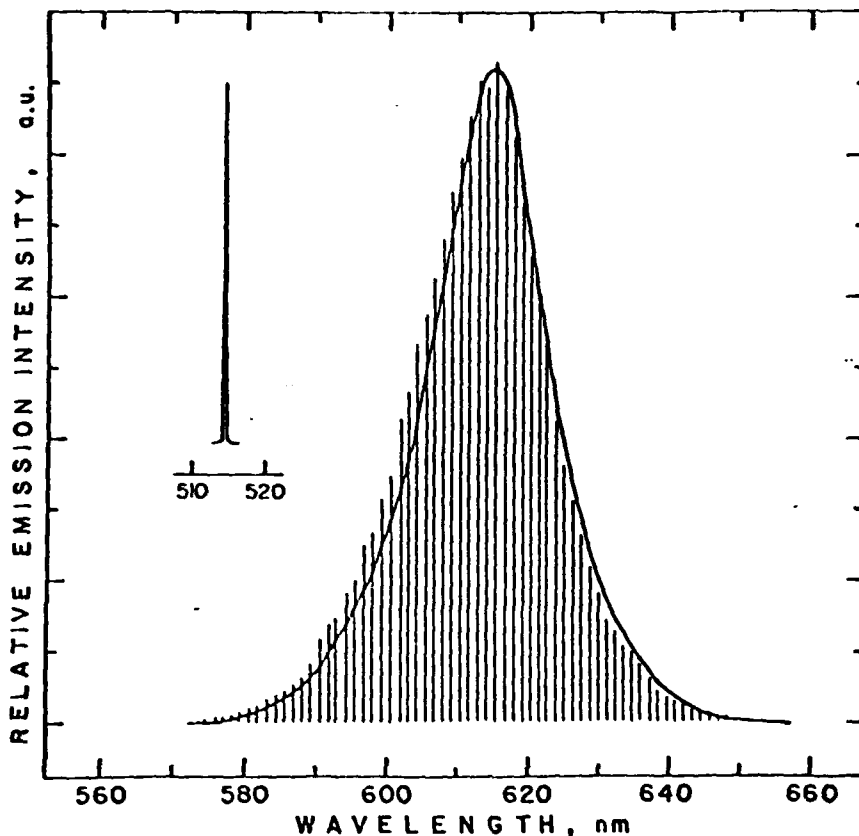


Figure 3. Uncorrected PL (solid curve) and EL (vertical lines) spectra of $\text{CdS}_{0.49}\text{Se}_{0.51}$ obtained in the same sample geometry. The PL spectrum was taken with the electrode immersed in 5 M NaOH electrolyte at -1.50 V vs. SCE. The 514.5 nm line of an Ar ion laser whose beam was expanded and masked to fill the $\sim 0.25\text{-cm}^2$ electrode surface was used for excitation; the excitation spike is shown in the inset. The EL spectrum was taken in 5 M NaOH/0.1 M $\text{K}_2\text{S}_2\text{O}_8$ electrolyte. The electrode was continuously pulsed between 0.00 V (11s) and -1.50 V vs. SCE (1s) while the emission spectrum was scanned at 6 nm/min. For both PL and EL a spectral resolution of 0.3 nm was employed. The EL spectrum has been scaled down to match the PL intensity at $\lambda_{\text{max}} \sim 615$ nm.

DATE
ILMEI
-8